1   Introduction

Many of the adverse outcomes of technologically important applications that involve fluid flows find their root in a fluid instability. Examples include shear layer instabilities that result in large acoustic levels (e.g., jet noise); boundary layer instabilities that lead to turbulence onset causing increased drag and surface heating, with the latter being extreme at hypersonic Mach numbers; unsteady flow separation behind bluff bodies (e.g., suspended cables, bridges, buildings, ground vehicles, etc.) that leads to large unsteady loads and extreme amplitude vibration; and even in turbulent boundary layers where instabilities in the laminar sublayer increase viscous drag and enhance turbulence production. However, flow control that *exploits* fluid instabilities can, with minimum energy input, produce beneficial effects. In the case of a free shear layer instability associated with jet noise, passive flow control involving trailing-edge geometries that modify the instability in basic flow is effective. If jet mixing is the objective, it can be substantially enhanced by introducing periodic disturbances that key on shear layer and jet core instabilities. An extreme example is "blooming jets" presented in Chapter 5 that was aimed at highly enhanced fluid mixing. Since free shear layers are associated with separated flows, introducing unsteady disturbances that cause the shear layer to accelerate turbulence onset is an effective method for flow reattachment. Bluff body flows discussed in Chapter 3 are in a special class as they can exhibit a global instability that is highly sensitive to even small modifications in the basic flow. As a result, passive modifications to near-wake bluff body flows have been especially effective.

1.1   Flow Control: An Instability Approach

Given these examples, the flow control approach embraced in this book is to recognize relevant fluid instabilities of a given flow field and then utilize them to seek to modify the flow to achieve a positive outcome. Figure 1.1 illustrates the basic physics of a fluid instability. It is important to understand that a fluid instability is that of the basic (time-independent) flow. An example of an unstable basic flow field that is illustrated in the figure is a free shear layer that exhibits an inflectional mean profile. The instability is promoted by unsteady disturbances from the environment. These disturbances might contain a broad spectrum of frequencies; however, the instability mechanism acts like a band-pass-filter amplifier that amplifies a selected band of

frequencies based on the basic flow. If the amplitudes of the environment disturbance are within levels assumed by linear stability analysis (generally below 1 percent of the maximum mean flow velocity), the amplified bands of frequencies are those whose integrated growth, or N-factor, is the largest based on linear stability analysis. Linear stability predicts that unstable disturbances grow exponentially in time or space. The amplification rate depends on the frequency or wave number.

In general, there exists a controlling parameter for a fluid instability that needs to be exceeded for disturbances to be amplified. In buoyancy-driven flows, this parameter is the Rayleigh number. In centrifugally driven flows, the parameter is the Taylor number. In open flows driven by either a pressure gradient or moving surfaces, the parameter is the Reynolds number. For any of these, there is a critical value below which linear disturbance will decay exponentially. The critical value depends on the disturbance frequency or wave number. The particular frequency or wave number with the lowest critical parameter value is called the minimum critical value. The right-most box in Figure 1.1 illustrates the amplitude response of a convective instability that is growing in space. R in this case is the Reynolds number based on a spatial development length scale, x, where then $R = Ux/\nu$. As illustrated, the amplitude of disturbances decays until the critical value, $R_{\mathrm{I}} = Ux_c/\nu$, is exceeded. Past the critical value, the amplitude increases, reaching a maximum and then decaying. In some flows, such as a Blasius boundary layer, there exists a second instability Reynolds number, R_{II}, beyond which linear disturbances decay. This does not exist in the example free shear flow. However, as the instability amplitude grows, it brings on nonlinear effects that generally cause the growth to asymptote. In some cases, the nonlinear effects include a mean flow distortion that triggers rapid turbulence onset.

Flow control approaches that utilize a fluid instability to amplify *controlled* disturbances perform best when they are introduced near the minimum critical value of the controlling parameter, for example, near R_I in a boundary layer. This approach can then fully exploit the region of exponential growth, as well as to not have to compete with instability modes resulting from uncontrolled background disturbances that may be more amplified than the controlled instability.

There are two basic approaches to flow control that are based on a fluid instability approach. These are illustrated in Figures 1.2–1.4. Since fluid instabilities are an instability of the basic (time-independent) flow, the first approach is to *modify the basic flow*. Figure 1.2 provides an example of this approach as applied to a free shear layer. In this example, a sinusoidal arrangement of peaks and valleys is added to the otherwise straight trailing edge of the flow splitter plate. The amplitude and spanwise wavelength of the peaks and valleys are parameters that could be selected based on linear stability analysis of the distorted mean flow. The general purpose of the sinusoidal trailing edge is to introduce streamwise vorticity that modifies the mean flow and therefore suppresses the growth of the initially most amplified two-dimensional (2-D) instability wave. As shown in Figure 1.3, this approach is widely used on the jet engines of commercial aircrafts to lower the sound levels that are intrinsically tied to the free shear layer instability. Other similar approaches described in Chapter 5 include spanwise-periodic chevron-shaped deformations of the trailing edge and
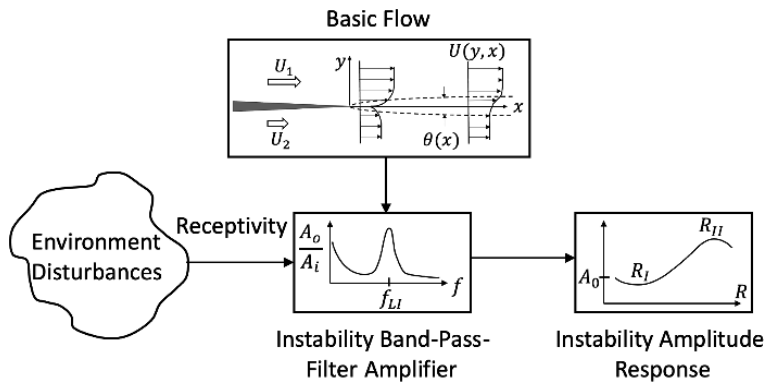
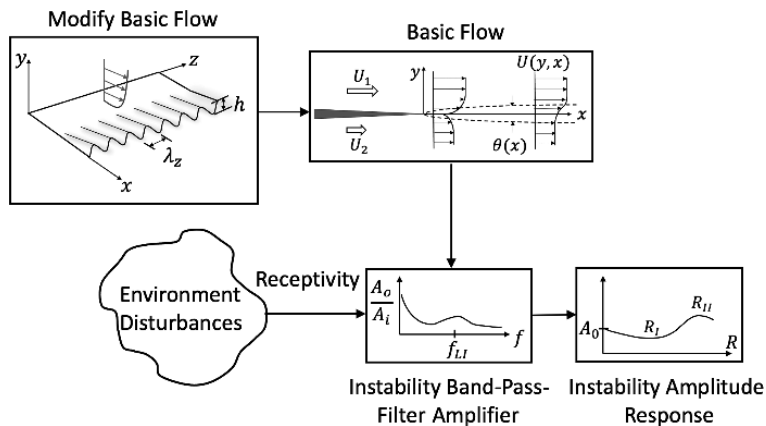**Figure 1.1** Illustration of a natural fluid instability process.

Figure 1.2 Example of an instability approach to flow control that involves a method that modifies the basic (time-independent) flow field.

surface streamwise vortex generators (VGs). In the free shear layer that exits from round jets, changes in the basic state have included introducing an azimuthal variation in the length of the jet nozzle to produce an azimuthal variation in the initial shear layer thickness. Since the shear layer instability frequency scales with the initial shear layer thickness, this modification of the mean flow can result in azimuthal bifurcations in the otherwise azimuthally contiguous (ring) vortices.

The second approach to flow control is based on *actively* interfering with the natural instability frequency, wavelength, or initial amplitude; for example, to introduce unsteady disturbances that either enhance or delay the growth of the natural instability. This approach is illustrated in Figure 1.4 which again considers the free shear layer as an example. In this case, disturbances with a prescribed amplitude and frequency are introduced through an oscillation of the trailing edge of the splitter plate. In the simplest case, the trailing-edge oscillation would not vary in the spanwise direction and
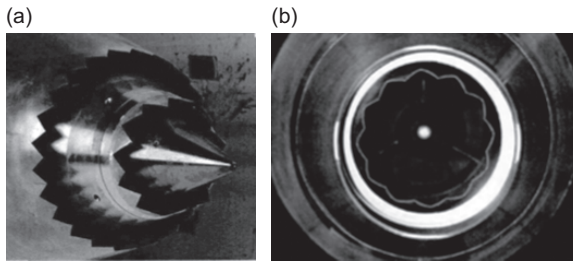
Figure 1.3 Application of shear layer flow control on commercial jet engines consisting of chevron-shaped cutouts (a) and surface-normal sinusoidal trailing edge (b). NASA Glenn Research Center photograph.
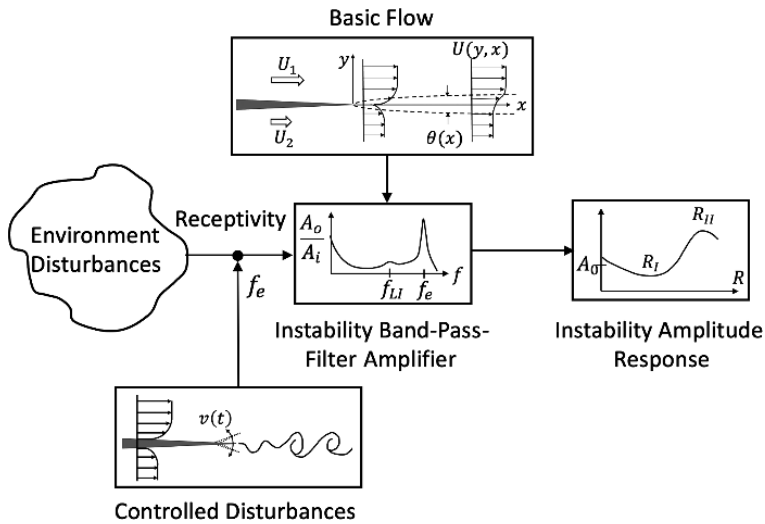

Figure 1.4 Example of an instability approach to flow control that involves a method that introduces an unsteady disturbance that can be amplified by flow field.

thereby would only introduce 2-D disturbances. At incompressible Mach numbers, the 2-D instability wave is most amplified. At compressible Mach numbers, three-dimensional (3-D) oblique waves are most amplified and would require controlled 3-D disturbances.

If the objective is to enhance the growth of the instability waves, the trailing-edge frequency should be close to the most amplified shear layer frequency based on linear stability theory. This would correspond to f_{LI} on the frequency axis of the amplitude spectrum shown in the middle of Figure 1.4. One quite spectacular example of enhanced growth of a 2-D free shear layer that dates back more than 150 years from Tyndall (1864) is shown in Figure 1.5. In this example, the introduction of a monochromatic sound source caused the gas jet to dramatically spread. As discussed in Chapter 5, acoustic pressure is transformed into equivalent motion of the trailing edge through an "acoustic receptivity" mechanism.

Figure 1.5 Images of a gas flame in a quiescent state (a) and when excited by monochromatic sound "whistle." (b) Taken from Tyndall (1864).

If the objective is to suppress the natural development of the shear layer instability, one approach involves introducing a disturbance at a frequency that is *less amplified*. In that case, by virtue of the controlled excitation, its higher initial amplitude can cause the less amplified excited mode to dominate over more amplified frequencies having lower initial amplitudes. This is illustrated in Figure 1.4, where f_e is the excitation frequency. The slower growing mode will eventually reach an amplitude where non-linear effects will emerge. This will include a modification of the mean flow, which will further suppress the possibility of the growth of more amplified frequencies.

The previous approach to instability control is an example of *open-loop* control. If, however, the amplitude of an instability wave is low enough to satisfy linear theory assumptions, it is possible to suppress its spatial growth by the addition of a second instability wave whose amplitude matches that of the oncoming wave, and whose periodic motion is phase-shifted by 180°. The approach is "linear phase cancelation." An example is illustrated in Figure 1.6 where an oscillating airfoil is placed within the shear layer at a downstream location. The airfoil oscillating motion would be selected to produce linear-amplitude vorticity waves that could linearly cancel the approaching shear layer instability wave. The effectiveness of linear phase canceling depends on the ability to match the amplitude of the incoming wave as well as to produce an opposing phase shift. This generally requires some form of closed-loop control.

Linear phase cancelation has mainly been attempted to control the growth of Tollmien–Schlichting (T-S) instability waves in low-speed boundary layers. Illustration examples are shown in Figure 1.7. In the setup shown in Figure 1.7(a), two vibrating ribbons are used to individually excite T-S waves (Schubauer and Skramstad, 1947). One ribbon is located at an upstream location near the T-S Branch I neutral growth curve. This ribbon is used to excite the primary T-S wave. The other ribbon is located some distance downstream where the T-S wave still exhibits linear growth. Knowing the amplitude and phase of the upstream vibrating ribbon motion, it is relatively easy to adjust the amplitude and phase of the downstream ribbon to cancel the incoming traveling wave. However, when the primary T-S wave results from uncontrolled background disturbances, the method is more challenging.
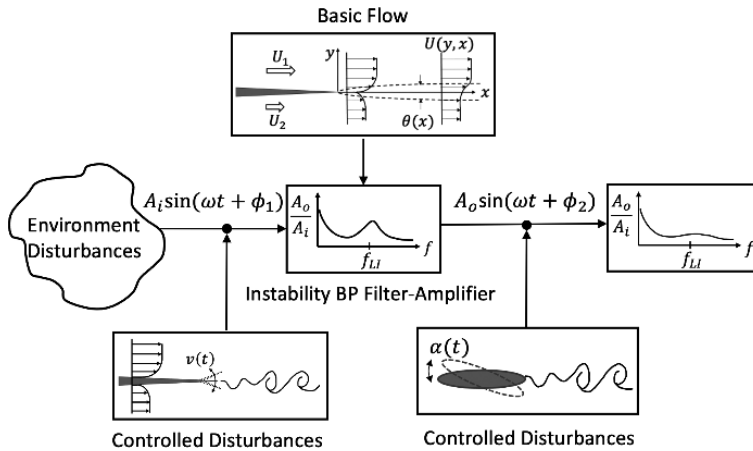
Figure 1.6 Example of an instability approach to flow control that involves linear phase canceling of a downstream traveling instability wave.

Phase cancelation attempts have also utilized sensors that were located upstream of the phase-canceling wave device. Figure 1.7(b) illustrates that approach. The upstream sensors are intended to measure the amplitude and phase of the incoming wave. A trained control system then constructs a conjugate waveform to be produced by the flow actuators to suppress the oncoming instability wave. In some cases, downstream sensors are used to measure the amplitude of any residual wave(s) to adjust the actuator motion while seeking to minimize any residual wave motion. Overall, with uncontrolled initial conditions, these approaches do not provide much benefit in delaying turbulence onset. A further complication in the attempts to phase cancel 2-D T-S wave is that even asymptotically small amplitude residual 2-D waves can interact with 3-D waves having the same phase speed that results in the resonant growth of the 3-D waves and turbulence onset (Craik, 1971).

The previous examples have focused on 2-D mean flows; however, in many applications, the mean flow is 3-D. The flow over a swept wing that is typical of most high-speed aircraft is an example of a 3-D mean flow that results in a cross-flow instability that dominates over other potential instabilities leading to turbulence onset (Saric and Reed, 2002). The cross-flow arises from a combination of pressure gradient and wing sweep that causes the inviscid-flow streamlines at the boundary layer edge to deflect inboard. The cross-flow boundary layer exhibits an inflectional mean velocity profile that is a characteristic of free shear layers and is inviscidly unstable. The cross-flow instability results in both traveling and stationary cross-flow modes. Although the traveling cross-flow modes are more amplified, the stationary modes are extremely sensitive to surface roughness, and generally dominate turbulence onset. The stationary modes appear as a regular pattern of corotating vortices that are easily visible in surface flow visualization or surface heat flux images. As an example, Figure 1.8 shows an image of the surface heat flux over a 70° swept fin at Mach 6 in which discrete roughness elements have been applied to excite stationary cross-flow
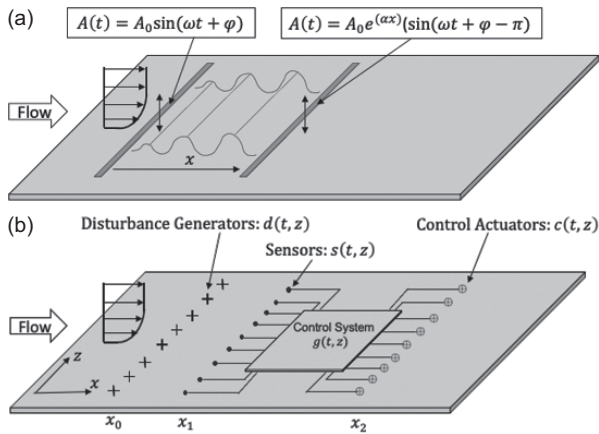
Figure 1.7 Examples of a laminar boundary layer 2-D (a) and (b) 3-D (b) T-S wave phase cancelation setup.

modes. The presence of the stationary cross-flow vortices is evident in the image by the periodic light and dark streaks that respectively correspond to regions of high and low surface heat flux.

Having this knowledge of the cross-flow instability, the approach to control the instability and subsequently delay turbulence onset involves introducing a controlled disturbance that will excite a less amplified mode that can dominate over other more amplified modes. In this case, it is done by applying discrete roughness having a wavelength that will excite a less amplified stationary cross-flow mode. This process, which was pioneered by Saric et al. (1998a), is illustrated in Figure 1.8. In that, the growth of the most amplified stationary cross-flow mode with "critical" wavelength λ_c is circumvented by the introduction of an evenly spaced discrete roughness with a wavelength, λ_{sc}. The growth of the less amplified stationary cross-flow modes ultimately inhibits the growth of the more amplified stationary modes by modifying the basic flow. Saric et al. (1998c) found that patterned surface roughness in the form of hemispherical "dots" with a height of 50 μm provided an effective transition delay in low-speed swept wing experiments. The method has also proved to be effective in experiments at Mach 3.5 (Schuele et al., 2013) and Mach 6 (Corke et al., 2018).

1.1.1   Free Shear Layers and Jets

In all of these examples, the flow control approach is tied to an instability of a specific basic flow that depends on such factors as (1) the flow condition such as the Mach and Reynolds numbers, (2) the geometry over which the basic flow develops, and (3) the receptivity of the basic flow to the disturbance environment. The examples in Figures 1.1–1.6 utilized a free shear layer to demonstrate basic flow control approaches that are linked to the control of a fluid instability. Free shear layers of the kind that are formed by the merging of two streams or a single stream into a quiescent fluid are
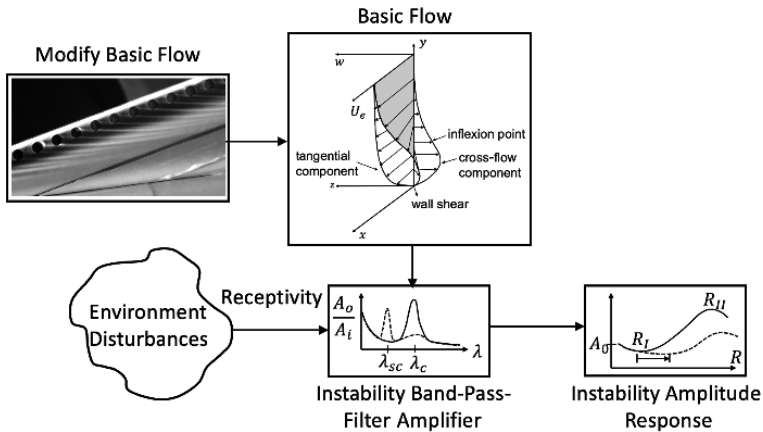
Figure 1.8 Example of an instability approach to flow control that involves a method that introduces an unsteady disturbance that can be amplified by flow field. Taken from Middlebrooks (2022).

simple flow configurations that arise in numerous natural phenomena as well as many engineered devices. In most of the engineered applications, the objective is to enhance fluid mixing.

One of the most striking and distinct features of free shear layers is the emergence of subharmonic components of the initial shear layer instability frequency. This results in a sequence of successive mergings (pairings) of the discrete vortices formed by the initial role-up of the instability wave. A visual example of this sequence was captured by Winant and Browand (1974). In this process, the mean vorticity of the basic flow is sequentially redistributed and spread across the shear layer. Controlled conditions that encourage the successive vortex pairings can greatly enhance shear layer spreading and mixing.

Ho and Huang (1982) observed that exciting a higher initial level fundamental shear layer frequency can temporarily suppress the growth of the subharmonic, frequency, and therefore delay vortex pairing. Similarly, when exciting a frequency, f_e, such that $f_n/3 < f_e < f_n/2$, the frequency that emerged in the shear layer jumped to the first harmonic, $2f_e$, that came closest to the natural fundamental shear layer frequency, f_n. In this case, the excitation became the subharmonic of the initial vortex passage frequency, and in contrast with the previous fundamental excitation, vortex pairing was promoted. Ho and Huang (1982) also documented that further reductions in the excitation frequency could lead to successive frequency-locking stages in which the resulting shear layer frequency became the second and third subharmonics of the excitation frequency, resulting in the coalescence of as many as three or four vortices. These results provide a prime example of efficient instability-based flow control. By this approach, Ho and Huang (1982) indicate that only very low excitation levels, on the order of 0.01–0.1 percent of $\overline{U}$, were required.

Acoustic pressure disturbances that occur in the formation and pairing of shear layer vortices can feed upstream and be felt at the splitter plate trailing edge, the

acoustic receptivity site. As a result, this pressure feedback can reenforce a narrow band of instability frequencies and lead to a feedback resonance. The sensitivity to acoustic disturbances increases with increasing trailing-edge sharpness (i.e., decreasing trailing-edge radius).

The most cited evidence of the feedback mechanism comes from Kibens (1980) in which the shear layer of a low Mach number axisymmetric jet was acoustically excited. The exit shear layers of round jets have all of the characteristics of 2-D shear layers when the ratio of the initial momentum thickness to the jet exit radius of curvature is small, $\theta/r < 0.01$. While smoothly scanning through a range of excitation frequencies, f_e, Kibens (1980) documented stair-step-like frequency "lock-in" regions corresponding to excitation frequencies $f_e, f_e/2, f_e/4$, and $f_e/8$ that were indicative of a feedback resonance. They indicated that the frequency stair-step jumps corresponded to vortex pairing events, which was consistent with the factor of two frequency changes at each jump.

In a somewhat surprising revelation, the evolution of vortical structures in *turbulent* shear layers is governed by essentially the same dynamical processes as their laminar counterpart. Brown and Roshko (1974) subsequently confirmed that large-scale coherent structures are indeed intrinsic features of turbulent mixing layers at high Reynolds numbers. Furthermore, sequential mergings of vortices provide the primary mechanism for the spreading of the layer in the downstream direction, as underscored by the experiments of Winant and Browand (1974).

A majority of the literature on shear layer instabilities, like those cited, have involved incompressible Mach number flows in which the most amplified instability modes are 2-D. At compressible Mach numbers, the most amplified instability modes in free shear layer are 3-D, or more specifically oblique waves. Instability control in this regime then focuses on introducing controlled 3-D disturbances. Some of the most successful approaches have involved passive modifications to the basic flow, again using 3-D ramps and tabs. In supersonic jets, the so-called intermediate-origin nozzles (Wlezien and Kibens, 1988) have been very successful in enhancing spreading and vectoring of the jet core flow. Active approaches are more limited, which has generally been due to the limits in flow actuator frequency response and/or amplitudes. However, some success has been reported by Samimi et al. (2007) using arc-filament plasma actuators.

1.1.2 Laminar Boundary Layers

In contrast to free shear layers, wall-bounded flows such as boundary layers and channel flows undergo a viscous instability. Although Taylor (1915) had previously indicated that viscosity can destabilize a flow that is otherwise stable, it remained for Prandtl (1921) to independently make the same discovery and set in motion investigations that led to a viscous theory of boundary layer instability. Any doubt that instability and transition to turbulence were synonymous in boundary layers was erased by the low value of its instability-critical Reynolds number. The seminal experiment of Schubauer and Skramstad (1947) fully demonstrated the existence

of instability waves in the boundary layer, their connection with turbulent transition, and the quantitative description of their behavior to the theory of Tollmien (1935) and Schlichting (1940). Although the instability waves are referred to as Tollmien–Schlichting waves, or T-S waves, based on their contribution in validating the theory, it might be fitting to refer to them as Tollmien–Schlichting–Schubauer–Skramstad waves.

The T-S modes are traveling vorticity waves. The waves can be 2-D or oblique. At subsonic Mach numbers, the 2-D waves have the lowest critical Reynolds number and are most amplified. At supersonic Mach numbers, this reverses, with 3-D waves being most amplified. In either case, the wave phase velocity is always less than the free-stream velocity so that at some height in the boundary layer, the mean velocity is equal to the phase velocity. The height at which this occurs defines the "critical layer," which plays a central role in the mathematical theory, as well as being *important in T-S wave control*.

The critical Reynolds number varies with frequency or wave number. Being a dispersive medium, different frequencies propagate with different phase velocities so that individual harmonic components in a group of waves will displace from each other over time. The group velocity can be considered to be a property of the individual waves. If an observer is moving at the group velocity, the wave in the moving frame of reference will appear to grow in time (temporal growth). In contrast, in the stationary frame of reference, the wave appears to grow in space. This insight yields a relation between temporal and spatial growth that is attributed to Gaster (1962).

A focus of boundary layer studies has been on predicting turbulence onset. The conjecture is that it occurs when the instability mode amplitude reaches a *critical* level. Linear stability theory can only predict the growth in amplitude, whereas the absolute instability *amplitude* can only be predicted when the initial amplitude is known. This disjoint led to a turbulence prediction method based on the spatial integration of the linear growth of a disturbance of arbitrary initial amplitude. The method, which is a hallmark for boundary layer turbulence onset prediction, is referred to as the e^N method. Values of N have come from experiments and range from 7 to 10.

The e^N method is extensively used in industry because its low computational overhead makes it suitable for iterative design approaches. The reason the method works is that in boundary layers, the development length of the linear instability process is long compared to that of the nonlinear development prior to turbulence onset. This reduces the sensitivity to the choice of N in these predictions based on this method. From a boundary layer transition control point of view, maintaining N values below those predicted from experiments can provide a metric of merit for preventing turbulence onset.

Boundary layer instability growth rates and N-factors strongly depend on the streamwise pressure gradient. Favorable pressure gradients stabilize the boundary layer, whereas adverse pressure gradients have a destabilizing effect. The former is the basis of laminar control airfoils whose section shape moves the maximum thickness point aft to maintain a favorable pressure gradient over a larger extent of the airfoil chord length.

In an effect similar to a favorable pressure gradient, wall-normal suction stabilizes boundary layers. Wall suction is even effective in stabilizing boundary layers that are close to separating and exhibiting highly unstable (inviscidly) inflectional mean velocity profiles. Conversely, similar to an adverse pressure gradient, wall-normal blowing destabilizes boundary layers. Braslow (1999) provides a history on the use of suction-type laminar flow control on flight research.

There are a wide range of *passive* boundary layer "tripping" techniques used to accelerate the streamwise development to a fully turbulent regime. These include distributed roughness particles, dimpled surfaces, and 2-D protrusions. A critical parameter for any form of roughness is the roughness Reynolds number based on a length scale that corresponds to the maximum roughness height that *does not affect* the turbulent onset location. The velocity used in the roughness Reynolds number is the friction velocity based on the wall shear stress at the location of the roughness.

The criteria for turbulent trips made up of distributed "sand paper" roughness are not as clear as that for 2-D roughness. For example, the roughness height can refer to the mean height of the particles, the peak height of the particles, or the root mean square of the roughness height distribution. From a boundary layer instability perspective, one might consider each roughness particle as an unsteady disturbance source with broad frequency content. These disturbances will be amplified according to the stability of the basic flow. By this perspective, the distributed roughness does not modify the mean flow. Rather, its effect is to increase the initial amplitude of disturbances that feed the T-S waves, causing them to reach nonlinear amplitudes in a shorter streamwise distance.

Active transition delaying approaches that have focused on linear phase cancelation have at best produced marginal results. The practical limitations of 2-D T-S wave cancelation for transition control were brought out in experiments by Thomas (1983). Although a reduction in the amplitude of the T-S wave was observed, smoke-wire flow visualization revealed that with the reduction in the plane T-S wave, 3-D waves emerged likely through a triad resonance mechanism predicted by Craik (1971).

In an attempt to account for the growing 3-D instability waves, Li and Gaster (2006) constructed a multi-input multi-output control system based on a 3-D array of sensors and actuators. The arrangement was shown in Figure 1.7(b). The control system was found to reduce but not completely cancel out the disturbance waves.

In an approach to minimize the computational overhead of a feedback boundary layer transition control system, Fan et al. (1995) utilized a neural network controller. Backpropagation (feedback control) from a sensor located downstream of the control actuator was used to train the neural network. Fan (1995) observed that with an initial training period of about 100 T-S cycles, almost complete T-S wave cancelation occurred. In addition, a low residual level could be maintained if the flow conditions change on a timescale that was larger than the initial training period.

In contrast to boundary layers at subsonic Mach numbers, in supersonic boundary layers, the most amplified T-S modes are *oblique* waves. The wave angles range from 45° to 75°, where the wave angle increases with increasing Mach number. In 2-D boundary layers up to slightly below Mach 5, the oblique T-S modes are most

responsible for turbulence onset. However, at approximately Mach 5, an inviscid insta-
bility first identified by Mack (1984) becomes dominant over the viscous instability
that governs the oblique T-S waves. The inviscid instability results in a family of 2-D
"Mack modes" whose mode numbers increase with increasing Mach number. Physi-
cally, the Mack modes correspond to sound waves that reflect inviscidly between the
solid wall and the relative sonic line in the boundary layer.

Both the T-S and second Mack mode amplification rates are sensitive to the wall
temperature, which provides a degree of instability control. Wall heating will increase
the amplification of T-S modes but decrease the amplification of Mack modes. The
reverse occurs with wall cooling.

Most of the instability control in 2-D hypersonic boundary layers has focused on
passive approaches. This is undoubtedly the result of the limitations of active distur-
bance actuators to produce frequencies (order of 500 kHz) needed to interact with
dominant second Mack mode waves. In addition to wall heating, examples of pas-
sive approaches include leading-edge bluntness, acoustic absorbing wall liners, and
strategically placed surface roughness or wall waviness.

Fedorov and Malmuth (2001) were the first to propose that the growth of the second
Mack mode could be suppressed through a suitably designed ultrasonically absorp-
tive porous coating. Based on an analytical model, they predicted that a 25 percent
porous coating having 10–20 blind pores per second mode wavelength would result in
a factor-of-two reduction in the second mode growth rate. Experimental validation of
the concept was first performed by Wartemann et al. (2011). This utilized the natural
porosity of a fiber-reinforced ceramic (carbon–carbon) material that was applied to
the surface of a 7° half-angle right-circular cone at Mach 7.5. The experiments docu-
mented a 70 percent reduction in the second mode amplitude compared to an uncoated
smooth surface.

In a related approach, it is known that CO_2 gas has acoustic damping properties,
which suggests that injection of the gas into the boundary layer could suppress the
growth of the second mode in a manner similar to acoustic absorbing liners. Evidence
of this was reported by Jewell et al. (2013) in which a gas mixture consisting of 50
percent air and CO_2 by mass was found to delay turbulence by 30 percent.

Another passive approach aimed at suppressing the growth of the second Mack
mode has involved the placement of 2-D roughness elements at the T-S/second mode
"synchronization point" where the phase speeds of the viscous and inviscid modes
are very close to each other (Federov, 1997). This was initially investigated through
numerical flow simulations (Duan et al., 2013) and validated in experiments at Mach
5 and 8 by Casper et al. (2016). The experimental test article consisted of a 7° half-
angle cone that was installed with a series of roughness strips. The effects of both
single and multiple roughness strips were investigated. The height of the roughness
strips was half of the boundary layer thickness, which was within the recommended
50–60 percent of the boundary layer thickness (Fong, 2017). Also as recommended
(Fong, 2017), the streamwise width of the strips was twice the boundary layer thick-
ness. When multiple strips were used, they were spaced 10 strip widths apart. The
results were mixed. At Mach 8, the experiment documented a reduction in the second
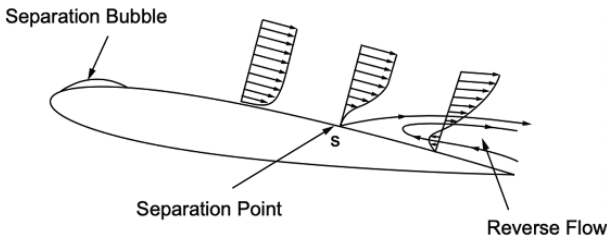
Figure 1.9 Example of flow separation that can occur on airfoils at moderate or large angles of attack.

mode growth. However, at Mach 5, the roughness strips effectively "tripped" the flow causing immediate turbulence onset.

1.1.3   Separated Flows

Boundary layer separation results when there is insufficient momentum in the flow to overcome an adverse pressure gradient or when viscous dissipation occurs along the flow path. Boundary layer separation is almost always associated with some form of aerodynamic penalty, including a loss of lift, an increase in drag, a loss of pressure recovery, and an increase in entropy. Although boundary layer separation is often viewed as 2-D and *steady*, experiments have shown the process to be strongly 3-D and highly unsteady. As with their free shear layer counterpart, the separated shear layer instabilities are highly receptive to external unsteady excitation, which is a characteristic that can be exploited in flow separation control.

In steady flows, boundary layer separation only occurs in regions of an adverse pressure gradient. As illustrated in Figure 1.9, the separation location corresponds to the stagnation point on the wall that separates the downstream moving and upstream moving (reverse) flows. The boundary layer velocity profile at that point exhibits an inflection that is therefore inviscidly unstable to external disturbances. These disturbances can be a combination of vortical and acoustic (pressure) fluctuations whose internal source could be convective instability waves if the upstream boundary layer is laminar or turbulent fluctuations if the upstream boundary layer is turbulent.

There are a number of boundary layer separation control methods that are aimed at increasing the momentum in wall-bounded flows. One of the most commonly used passive devices is a VG. VGs are designed to introduce coherent streamwise vortices that transport high momentum fluid from the free-stream toward the wall. Passive VGs generally consist of a row of small plates or airfoils that are mounted on the wall surface and set at an angle of incidence to the local mean flow direction. In early applications of VGs used for separation control, their height was on the order of the boundary layer thickness. Kuethe (1972) developed and examined nonconventional "vane-type" VGs with heights that were from 42 percent to only 27 percent of the boundary layer thickness. Rao and Kariya (1988) suggested that passive VGs with $h/\delta \leq 0.625$ could be just as effective in flow separation control but with much lower

parasitic device drag. Lin (2002) subsequently provided an in-depth review of these "low-profile VGs."

There are a number of active approaches that produce an effect similar to a passive VG. One of the simplest of these involves angled wall jets. For example, a single streamwise vortex in either circulation direction can be generated by angling a wall jet in either cross-stream direction. Pairs of angled jets can emulate the effect of a passive vane-type VG. For these, jet velocities that were 80 percent of the free-stream velocity have been found to be effective in controlling boundary layer separation (Johnston and Nishi, 1990).

The previous approaches can be used to both *prevent* flow separation as well as to *cause* a separated flow to reattach. In these cases, the flow control is aimed at modifying the mean (basic) flow.

In the case of an already separated flow, the instability characteristics of the separated shear layer offer a low-energy active approach to reattach the flow. For example, it has been demonstrated (Seifert et al., 1996) that oscillatory blowing introduced just upstream of the separation point is an effective means of reattaching the flow. In this, an important observation was that the most effective excitation frequency was the one having a reduced frequency, F^+, that scaled with the length of the separated flow region and local free-stream velocity of which the optimum was $F^+ = 1$. In this case, the optimum excitation frequency clearly acted on a separated shear layer instability mechanism. Assuming that the separated shear layer mean profile has a representative hyperbolic-tangent velocity distribution, then linear stability analysis predicts a wave phase speed of $c_r = 0.45 U_\infty$. For the optimum reduced frequency, $\omega L/U_\infty = 1$, in which L is the length of the separated region, and noting that the frequency of the traveling waves is $\omega = c_r/\lambda$, where λ is the wavelength, the optimum frequency to attach a separated flow corresponds to that in which there are two instability wavelengths spanning the separated flow region. With regard to methods for introducing the periodic disturbances for flow separation control, they have included acoustic excitation (Nishioka et al., 1990; Nishizawa et al., 2003) and a periodic body force produced by a pulsed plasma actuator (Kelley et al., 2014).

The receptivity of the separated shear layer to external or internal disturbances and controlled excitation can be exploited to provide a method for detecting separation onset. For example, in the analysis of acoustic receptivity of a boundary layer over a parabolic leading edge, Haddad et al. (2005) found that there was a 100-times growth in the receptivity coefficient just prior to flow separation. As a result, just prior to flow separation, the boundary layer is significantly more responsive to the disturbances (background or controlled). Based on this, He (2008) and Lombardi et al. (2013) devised a flow separation detection approach that became an integral part of a closed-loop separation control system. The approach utilized a pressure sensor located a short distance downstream of the leading edge on the suction side of an airfoil. A periodic disturbance (perturbation) was introduced upstream of the pressure sensor location. At low airfoil angles of attack where the flow remained attached, the amplitude of the perturbations sensed by the pressure transducer was low. However, when the angle of attack was increased to just before the flow would separate, as a result of the enhanced

receptivity of the boundary layer, the perturbations sensed by the pressure transducer significantly increased. The method thus provided an indication of the incipient flow separation. In a closed-loop control system, the indication of imminent flow separation could then initiate any of the separation control approaches previously discussed.

1.1.4   Shock–Boundary-Layer Interaction

Shock–boundary-layer interactions (SBLI) appear in numerous high-speed flows including those of supersonic engine intakes, transonic gas turbine blade tip gaps, transonic turbine blade passages, scramjet isolator ducts, transonic and supersonic flight vehicle surfaces, and surfaces of rockets, missiles, and reentry vehicles. It is of particular interest because it can greatly affect the boundary layer development including causing large temporal and spatial pressure fluctuations and *flow separation* that greatly affects aerodynamic performance.

A schematic that illustrates the features of an incident oblique shock wave interacting with a wall boundary layer is shown in Figure 1.10. The incident shock can originate either from an external surface above the wall or from a shock wave that reflected from an upper wall as part of a duct. If the incident shock is sufficiently strong, the pressure gradient across the shock can cause the boundary layer to separate, forming a recirculating separation bubble. The separation bubble causes the mean flow to deflect away from the wall. This results in an adverse pressure gradient that communicates upstream through the subsonic portion of the boundary layer to a point where a "reflected" shock is formed. The location of the reflected shock is well upstream of where it would have been located if the flow were inviscid. Finally, an expansion fan forms over the top of the separation bubble. This is quickly followed by compression waves that form near where the separated flow reattaches. Further downstream, the boundary layer can gradually return to a fully developed equilibrium condition. However, depending on the size of the separation bubble, the downstream distance needed to reach equilibrium can take an order of 10–20 boundary layer thicknesses.

Wall cooling can reduce the effect of the adverse pressure gradient that forms downstream of the incident shock and thereby delay or reduce the extent of boundary layer flow separation (Kepler and O'Brien, 1962). In a turbulent boundary layer, if the ratio of the wall temperature to recovery temperature is less than 1, it will lower the viscosity compared to an adiabatic wall condition. This has the effect of increasing the local Reynolds number and increasing the wall shear stress, similar to adding momentum near the wall. By the same arguments, heating the wall has the opposite effect and can therefore hasten flow separation.

Strategic wall suction has shown some benefits toward alleviating the adverse effects of a SBLI. If applied downstream of an impinging shock, the increase in the wall shear stress in the thinned boundary layer can offset the adverse pressure gradient produced by the incident shock, and thereby limit the formation of the separation bubble. Experiments at Mach 2.8 and 3.78 (Mathews, 1969; Seebaugh and Childs, 1970) indicated that suction levels from 2-5 percent of the mass flow of the approaching boundary layer were sufficient to prevent flow separation.
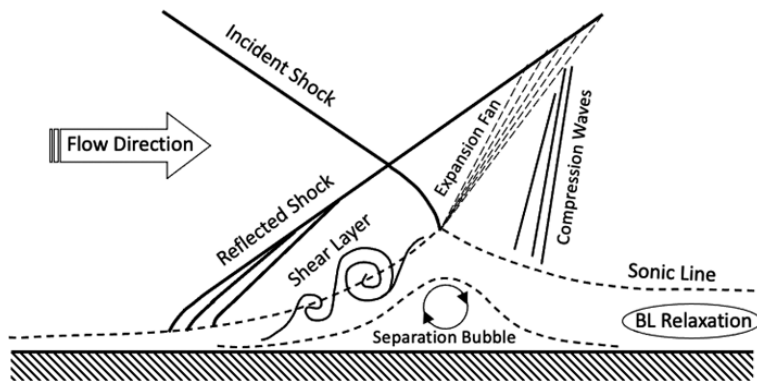
Figure 1.10 Schematic illustration of features of an incident oblique shock wave interacting with a wall boundary layer.

Wall suction applied upstream of the impinging shock could have a detrimental *or* a beneficial effect. Wall suction that thins the approaching boundary layer will move the sonic line closer to the wall and thereby make the shock near the wall stronger. This could more strongly promote flow separation downstream of the shock and commensurate flow unsteadiness. However, based on the "sonic point criterion" (Li, 2007), the stronger oblique shock would be more stable and thereby be less receptive to unsteady disturbances. Assuming that the flow unsteadiness that occurs from SBLI is due to an instability of the incident shock, then the thinning of the approaching boundary layer would reduce the unsteady shock motion.

One passive SBLI control approach exploits the pressure gradient across the shock (Barn et al., 1983). This approach locates a wall cavity covered by a porous screen under the impinging shock. The concept is that the pressure difference across the incident shock will circulate a flow through the cavity and exit upstream of the incident shock where it will energize the incoming boundary layer. Another passive approach involves the placement of wall-mounted streamwise VGs upstream of the incident shock. The intent is to enhance mixing throughout the boundary layer and thereby reduce the potential for incident shock-induced flow separation. McCormick (1993) performed a comparison of the effectiveness of the two techniques. The conclusion was that the covered wall cavity performed better at reducing the pressure loss across the incident shock.

With the same objective for the use of passive VGs, Souverein and Debieve (2010) investigated the use of a spanwise array of angled wall jets as an active approach to introduce streamwise vortices into the boundary layer for SBLI control in a Mach 2.5 flow. The wall-jet array was located five boundary layer thicknesses upstream of the incident shock location. The mass flow of the jet array was about 3 percent of the mass flow of the boundary layer. As expected, the angled jet array acted to thicken the approaching boundary layer. This was found to reduce the size of the shock-induced separation bubble but not to eliminate it.

Valdivia et al. (2009) sought to improve the effect of vortex generating wall jets by combining them with passive VGs with the specific motivation was to control "unstart" in an scramjet inlet isolator at Mach 5. The passive VGs were located upstream of the wall jets. Although each type of VG was effective by themselves, the combination of the two was found to be most effective with the reason being that the passive VGs mitigated the blockage produced by the bow shock that otherwise formed upstream of the wall-jet orifices.

Narayanaswamy et al. (2012) investigated the use of pulsed plasma-jet actuators as a replacement for air-driven wall jets. Two wall-jet orientations were examined: one in which the jet injection was normal to the wall surface, and another in which the injection angle was pitched and skewed to match a previously used orientation of air-driven wall jets (Souverein and Debieve, 2010). A spanwise array of three plasma jets was located six boundary layer thicknesses upstream of the reflected shock. The pulsing frequency corresponded to a Strouhal number that matched that of the characteristic unsteadiness associated with an SBLI. This was found to reduce the magnitude of pressure fluctuations by 30 percent.

In an approach that more directly utilizes the electro-magneto-hydrodynamics properties of the ionized air (plasma), experiments have been performed in which the electrodes are exposed to the primary flow and operated to generate long plasma filaments that extend downstream. In this arrangement, the primary function of the plasma discharge is to generate heat that locally lowers the Mach number and thereby weakens the incident shock strength (Leonov et al., 2010). Wang et al. (2009) combined the plasma filament generation with a magnetic field in order to seek to enhance the control of SBLI. The addition of a magnetic field coupled with the plasma discharge current results in a Lorentz force that can act on the flow field. In SBLI experiments at Mach 2.2 (Wang et al., 2009), the incident shock strength was reduced by as much as 11 percent.

All of the previous SBLI control approaches have focused on the boundary layer approaching the incident shock with the general intention of weakening the incident shock in order to reduce the strength and size of the flow recirculation bubble that forms downstream of the shock. However, a number of techniques used to generally control boundary layer separation can be applied. One example is steady wall-tangential blowing. Applying this approach to a shock-induced separation bubble, Viswanath et al. (1983) found that the distance to reattachment was significantly reduced.

1.1.5   Bluff Body Wakes

A bluff body can generally be categorized as one in which its length in the flow direction is approximately the same as its height perpendicular to the flow in a 2-D representation. Such shapes exhibit a wide wake on the scale of the body (2-D) height, and aerodynamic drag that is dominated by the low-pressure region that forms in the near wake of the body. Bluff body wakes are complex, involving boundary layer separation and multiple shear layer interactions.

The most widely studied bluff body shape is a large aspect ratio (2-D) circular cylinder. The flow around a circular cylinder can be considered as a prototype of bluff body wakes because of the simplicity of the boundary conditions and the complexity of the physical processes involved. A boundary layer over the cylinder surface originates at the upstream (windward) stagnation point. The boundary layer eventually separates as it approaches the adverse pressure gradient that exists near the downstream (leeward) side of the cylinder. The separation location will depend on the Reynolds number and surface roughness that determine whether the boundary layer state is laminar or turbulent. A low-pressure region is formed between the pair of separated shear layers. This low-pressure region includes a symmetric pair of flow recirculating cells. The flow recirculation in these cells has implications on the global stability of the wake flow.

A hallmark of bluff body wakes is the unsteady vortex shedding. von Kármán (1912) analyzed the stability of vortex street configurations and established a link between the vortex street structure and the aerodynamic drag. The relation between the vortex shedding frequency to the cylinder diameter and external flow conditions is attributed to the classic early experiments of Strouhal (1878). Investigations on the relation between the Strouhal number and the Reynolds number (Kovasznay, 1949; Roshko, 1954) led to characterizing three Reynolds number ranges: "Stable" $40 < \mathrm{Re}_D < 150$, "Transitional" $150 < \mathrm{Re}_D < 300$, and "Irregular" $300 < \mathrm{Re}_D < 10,000+$. Over a range of cylinder diameter Reynolds numbers where the separated shear layers are laminar, the Strouhal number is relatively constant with a value of 0.21. This is referred to as the "subcritical" Reynolds number range.

A general characteristic of bluff bodies is that the pressure or wake drag is much larger than the viscous drag of boundary layers over its surface. Morkovin (1964) found that the overall drag coefficient was inversely proportional to the Strouhal number. The drag coefficient abruptly changes for $\mathrm{Re}_D > 200,000$, which is where the previously laminar separated shear layers become turbulent. This results in an abrupt contraction of the near-wake width that results in a substantial decrease in the drag coefficient referred to as the "drag crisis." In general, the separated boundary layer and resulting free shear layers that develop off of the cylinder are convectively unstable. Therefore, any disturbances that would excite instabilities of the shear layer will amplify with downstream distance.

Landmark transient experiments (Mathis et al., 1984; Strykowski, 1986) have indicated that at low Reynolds numbers, the vortex shedding results from a global instability. As a result, disturbances grow in space and time rather than in space alone as with a convective instability. This has profound implications with respect to the control of low Reynolds number bluff body flows.

For example, Strykowski (1986) demonstrated that the addition of a small *control* cylinder into the near-wake region of a circular cylinder could completely suppress the vortex shedding. The addition of the control cylinder is thought to introduce asymmetry in the basic flow that changes the local stability properties of the wake, particularly those governing the absolute instability. Resistively heating the control cylinder was found to dramatically widen the region of vortex shedding suppression (Strykowski and Sreenivasan, 1990).

One of the most common methods to suppress the wake shedding is with the addition of a splitter plate. This has included single and segmented rigid and flexible plates. In most cases, these have been attached to the trailing portion of the cylinder. Investigations by Roshko (1954) on the streamwise placement of splitter plates to suppress vortex shedding of cylinders in the subcritical Reynolds number range found them to be effective when placed as far as four cylinder diameters downstream. Within that range, the effective length of the bluff body extended to the trailing edge of the splitter plate (Roshko, 1954). As a result, the process can be considered as "virtual streamlining."

Cardell (1993) studied the effect of a *permeable* splitter plate on cylinder wake. He noted that a permeable splitter plate that was carefully chosen to minimize geometrical effects would interfere with communication across the wake center plane, and by varying the permeability, it was possible to vary the magnitude of the interference created by the splitter plate. Hinged-rigid splitter plates have been recently studied (Assi et al., 2009; Shukla et al., 2009). For these, the control parameter is the damping in the hinge motion. With a relatively large hinge damping (Assi et al., 2009), the splitter plates did not oscillate but assumed a stable position at an angle to the flow direction, somewhat like a rigid plate. This was found to effectively suppress the wake shedding and provide a commensurate amount of drag reduction.

Shukla et al. (2013) considered the effects of a *flexible* splitter plate. In that case, the control parameter was the flexural rigidity (EI) of the splitter plate. Two Reynolds number regimes of periodic oscillations of the flexible splitter plate were observed. Within the two regimes, the normalized tip oscillation frequency was close to the natural (subcritical Reynolds number regime) Strouhal number (0.21). The bounds of these regimes depended on the amount of flexural rigidity.

Another of the early methods of bluff body wake control is "base bleed," in which some fraction of fluid is injected at the aft part of the body. An early demonstration (Wood, 1964) of the effect of base bleed on an airfoil blunt trailing edge produced a suppression of vortex shedding along with a substantial drag reduction. The critical bleed coefficient was found to be in good agreement with stability calculations (Monkewitz and Nguyen, 1987) that showed the wake to be everywhere convectively unstable below the critical value.

A number of active bluff body flow control approaches have involved the introduction of unsteady disturbances on the body. This has included surface motion using a piezoelectrically active actuator (Wehrmann, 1967), an unsteady 2-D slotted surface jet (Huang, 1996), and single dielectric barrier discharge plasma actuators (Thomas et al., 2008). In each approach, the choice of excitation frequencies could either suppress or reenforce the natural wake vortex shedding. These experiments have generally focused on the subcritical Reynolds number regime where the shedding Strouhal number is nearly constant, and the separating shear layers are laminar.

On circular cylinders, the most sensitive location to introduce controlled unsteady disturbances is just upstream of where the shear layers separate from the cylinder surface. In the subcritical Reynolds number regime, shear layer separation occurs at an approximate angle of 85° (measured from the stagnation line) or just forward of
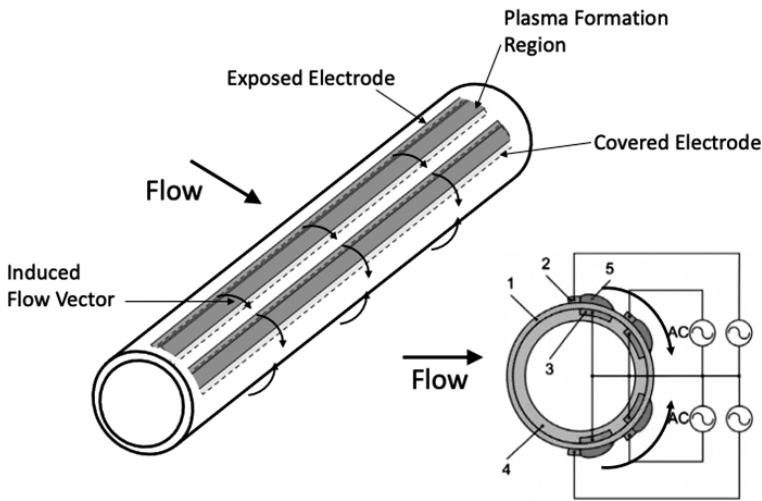
Figure 1.11 Illustration of four single dielectric barrier discharge plasma actuators used for active cylinder wake control. Taken from Thomas et al. (2008).

the cylinder apex. If periodic excitation is applied near that location, it can cause the shear layer separation location to oscillate, providing significant amplification of the disturbance amplitude.

Figure 1.11 shows an example of an arrangement of plasma actuators used to control vortex shedding of a 2-D circular cylinder. The cylinder had four plasma actuators located at $\pm 90°$ and $\pm 135°$ from the stagnation line. The plasma actuators were designed to induce a velocity component that was tangent to the cylinder surface and directed toward the downstream side of the cylinder.

Exploring a range of unsteady frequencies, Thomas et al. (2008) found that an optimum excitation frequency to suppress vortex shedding and subsequently to maximize the drag reduction occurred for an actuation frequency corresponding to $St = 1$, or five times the natural shedding Strouhal number (0.21) for a cylinder in the subcritical Reynolds number regime. Examples of the wake structure under this excitation condition are shown in Figure 1.12, where (a) corresponds to the symmetric shedding condition in which the top-half and bottom-half plasma actuators are operating in phase and (b) corresponds to alternate shedding condition where the top-half and bottom-half plasma actuators are operating with a 180° phase shift. In both cases, the flow visualization indicates that the vortex street has been completely suppressed. Thomas et al. (2008) indicated that the effect persisted well beyond eight cylinder diameters downstream.

1.1.6   Turbulent Boundary Layers

Flow control strategies for turbulent boundary layers have generally focused on either removing or altering in some way mechanisms underlying coherent motions that have
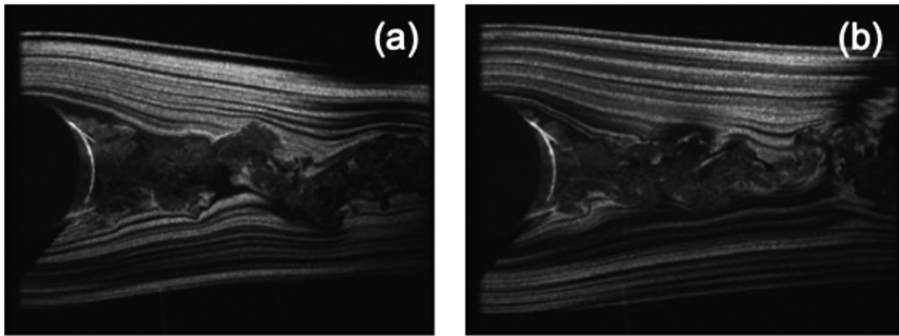
Figure 1.12 Flow visualization of the cylinder wake at $\mathrm{Re}_D = 3.3 \times 10^4$ with unsteady plasma actuations to excite symmetric shedding (a) and alternate shedding (b) at five times the natural Strouhal number, St = 1. Taken from Thomas et al. (2008).

been shown to contribute to sustaining turbulent energy production. This has generally involved either modifying the large vortical motions in the outer half of the boundary layer or modifying the small-scale vortical motions that occur in the lower third of the boundary layer, near the wall. Both passive and active flow control approaches have been examined and led to varying degrees of success.

In a landmark study using flow visualization, Kline et al. (1967a) observed surprisingly well-organized vortical motions in the near-wall region of a turbulent boundary layer. This appeared as a coalescence of the visualization markers into long streamwise oriented "streaks." Figure 1.13 provides an example image, where the flow direction is from the top. The spacing between the "streaks" was found to scale with the wall shear velocity, u_τ. Kline et al. (1967a) observed that the coherent streaks underwent a process of "gradual lift-up, sudden oscillation, bursting and ejection." This sequence became simply known as "bursting" and was felt to play an important role in the production of turbulence in the wall and buffer layers. Of singular importance, Kline et al. (1967a) noted a linear dependence of the viscous drag on the frequency of the bursting events.

The connection between the organized streamwise vorticity within the buffer layer and skin friction drag of turbulent boundary layers has been noted by Kim (2011). In this scenario within the buffer layer, coherent streamwise vortices transport near-wall fluid toward the wall on one flank and eject fluid away from the wall on the other flank. The wall-directed motions give rise to the so-called splatting events that steepen gradients of mean velocity, thereby resulting in higher time-mean friction drag. As noted by Schoppa and Hussain (1998a), the velocity gradient reduction effect of the outward directed motion is small in comparison to the enhancement of the velocity gradient produced by the wall-directed motion.

A general consensus has emerged (Jimenez and Moin, 1991; Waleffe et al., 1993; Hamilton et al., 1995; Jimenez and Pinelli, 1999), which is of an autonomous cycle for turbulence production involving the generation, growth, and instability of coherent streamwise vortices associated with the wall-layer "streak" structure. As part of
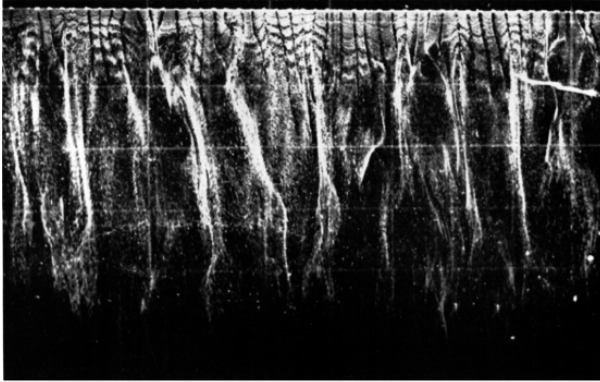
FIGURE 10b. $y^+ = 4 \cdot 5$.

Figure 1.13 Flow visualization of wall-layer "streak" structure first discovered by Kline et al. (1967a).

this, Schoppa and Hussain (2002) demonstrated that near-wall turbulence production may originate from a sinuous instability of the coherent streamwise vortices through the process of "streak transient growth." A critical parameter to the instability is the wall-normal vorticity, ω_y, that flanks the coherent streamwise vortices.

An idealized diagram of an autonomous cycle based on a "streak transient growth" is shown in Figure 1.14. This begins with the quasi-steady coherent streamwise vortices associated with the wall "streak" structure. The pumping action of the coherent vortices results in a spanwise mean flow distortion (thickening and thinning) of the buffer layer that results in elevated levels of the wall-normal vorticity, ω_y. The levels of ω_y eventually reach a critical value that triggers a sinuous instability of the streamwise vortices causing them to distort, lift up, and break up in the process described by Kline et al. (1967a). Following their breakup, the cycle begins again with the next generation of coherent wall-layer streamwise vortices.

Active flow control that focuses on disrupting this autonomous turbulence production cycle has focused on reducing the spanwise distortion produced by the coherent wall-layer streamwise vortices. This directly focuses on reducing the levels of ω_y to below the critical value of the sinuous instability. The approach is therefore one that acts to modify the basic state. Since this process of vortex lift-up and break-up was also linked to the viscous drag (Kline et al., 1967a), the stabilization would also result in drag reduction.

Schoppa and Hussain (1998) demonstrated drag reduction in a Direct Navier Stokes simulation of a turbulent channel flow in which they imposed a spanwise velocity component along the channel wall through either a pair of counter-rotating streamwise vortices or opposed wall jets. Both approaches resulted in significant drag reduction. Corke et al. (2017) and Thomas et al. (2016) demonstrated unprecedented levels of drag reduction of up to 70 percent by applying a mean spanwise velocity component at the wall using an array of plasma actuators. Measurements by Duong (2019) confirmed that this also resulted in a significant reduction in the frequency of "burst" event, the turbulent Reynolds stresses, and turbulence production.
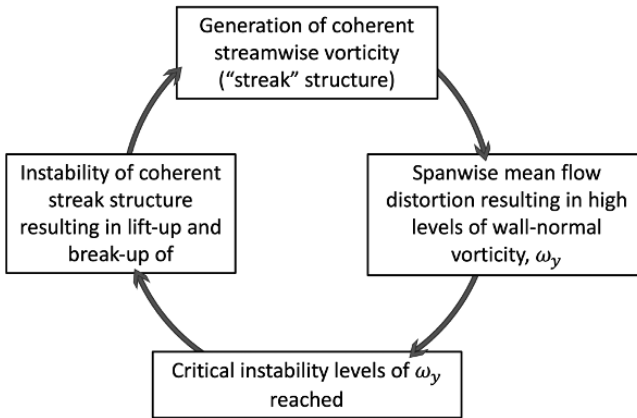
Figure 1.14 Autonomous wall-layer turbulence production cycle based on the concept of streak instability.

There are a large number of active and passive flow control approaches that focus on other mechanisms associated with coherent vortical structures in turbulent boundary layers. These are extensively covered in Chapter 8.

1.1.7   Flow Control by Design

In most cases, flow control is applied to an existing geometry that determines the basic flow. This can constrain flow control methods that are based on utilizing flow instabilities. As previously discussed, it is possible and sometimes advantageous to modify the basic flow through changes in the geometry. Examples included trailing-edge waviness, and the addition of passive elements such as splitter plates, VGs, ramps, cavities, and steps. In many of the previous examples, modification of the mean flow was used to prevent the growth of a fluid instability.

"Flow Control by Design" takes a broader approach in which a geometry is modified to make it more *receptive* to flow control that utilizes fluid instabilities. As an example, Patel et al. (2006) modified the trailing edge of an airfoil section by adding a 20° convex ramp that would cause the boundary layer to separate at that location. As presented earlier, a separated flow is highly receptive to disturbances and easily made to reattach through controlled periodic excitation. When the ramp was located on the pressure side of the airfoil, the separated flow at the trailing edge acted like a deflected trailing edge flap, increasing the aerodynamic lift. The added lift was removed when the separation bubble was forced to reattach. The result was lift control without a moving surface.

With the growing ability of computational fluid dynamics, it is now possible to formulate simulations that can systematically investigate multiple parameters that lead to a design that meets specific performance metrics. One approach utilizes an adjoint formulation of the Navier–Stokes (N-S) equations. The adjoint method has gained

much attention as an efficient sensitivity analysis method for aerodynamic optimization because it allows one to calculate sensitivity information *independently* for each of the design variables. Some early examples applied to the design of high-lift wing sections include that of Nielson and Anderson (1999), Kim et al. (2001), and Jameson (2003).

In a flow control approach based on utilizing flow instabilities, such adjoint N-S formulations can be used to seek geometric modifications that can enhance the receptivity of a basic flow to controlled disturbances, and thereby maximize flow control authority. Such capability might be the ultimate expression of "Flow Control by Design."